Supplemental Data:

Application of static modeling in the prediction of *in vivo* drug-drug interactions between rivaroxaban and anti-arrhythmic agents based on *in vitro* inhibition studies

Eleanor Jing Yi Cheong, Janice Jia Ni Goh, Yanjun Hong, Gopalakrishnan Venkatesan, Yuanjie Liu, Gigi Ngar Chee Chiu, Pipin Kojodjojo and Eric Chun Yong Chan

Drug Metabolism and Disposition

Supplemental Methods:

Measurement of Residual Enzyme Activity and Rivaroxaban Metabolite Formation via LC/MS/MS. All samples were analyzed using an Agilent 1290 Infinity ultra-high pressure liquid chromatography (UHPLC) (Agilent Technologies Inc., Santa Clara, CA, USA) interfaced with the AB SCIEX QTRAP 5500 tandem mass spectrometry (MS/MS) system (AB SCIEX, Framingham, MA, USA). Separation was performed on an ACQUITY UPLC BEH C_{18}, 1.7 µM, 2.1 × 50 mm column (Waters, Mildord, MA, USA). The column and sample temperatures were maintained at 45°C and 4°C respectively. Samples were delivered using an injection volume of 5 µL. The aqueous mobile phase (A) was 0.1% [v/v] formic acid in milli-Q water whereas the organic mobile phase (B) consisted of 0.1% formic acid [v/v] in ACN. Mobile phases were delivered at a flow rate of 0.6 mL/min. The gradient program was as follows: linear gradient from 25% to 95% B (0-1.21 min), isocratic at 95% B (1.21-2 min), linear gradient from 95% to 25% B (2-2.01 min) and isocratic at 25% B (2.01-2.5 min). All analyses were performed in ESI positive mode. The MS source conditions were as follows: source temperature 650°C, curtain gas 20 psi, ion source gas 1 (sheath gas) 45 psi, ion source gas 2 (drying gas) 60 psi, ion spray voltage +5000V, collision gas (nitrogen) medium. The compound-dependent MS parameters are summarized in **Supplemental Table 1**. Chromatographic peak integrations were performed with Analyst software ver. 1.6.2 (Applied Biosystems).

Kinetics and linearity of transport of rivaroxaban by P-gp. To determine the optimal incubation time for the transwell assay, 10 μM of rivaroxaban was tested for both A→B and B→A transport by sampling 200 μL of receiver solution at 0, 60, 90, 120 and 180 min. The samples were stored at -20°C for further processing prior to LC/MS/MS analysis. The P_{app} in each direction was determined and plotted against time. The optimal incubation time was selected when bidirectional P_{app} (A→B, B→A) of rivaroxaban demonstrated a linear correlation with time. To determine the optimal concentration of rivaroxaban, P_{app} (A→B) and P_{app} (B→A) were measured at increasing rivaroxaban concentrations (10, 20 30, 50 and 100 μM). An optimal concentration of rivaroxaban was defined as a concentration where P_{app} (B→A) was consistent, indicating non-saturated P-gp transporters. After a 90 min incubation, 200 μL of receiver solution was aliquoted into a 2 mL Eppendorf tube and stored at -20°C for further processing prior to LC/MS/MS analysis.

Time- and concentration- dependent optimization of MDCK-MDR1 Transport Assay. From 90 to 180 min, the gradient for A→B rivaroxaban transport started to plateau (**Supplemental Figure 1A**). On the other hand, B→A transport of rivaroxaban was linear from 0 to 180 min (**Supplemental Figure 1B**). Hence, 90 minutes was chosen as the optimal incubation time due to the linearity of rivaroxaban transport bidirectionally, indicating that dynamic equilibrium has not been attained. Over the concentration range of 10 to 100 μM rivaroxaban (**Supplemental Figure 2**), the efflux ratio of P_{app} (B→A) to P_{app} (A→B) was relatively consistent, indicating that rivaroxaban efflux was not saturable within the concentration range tested. A low concentration of 10 μM rivaroxaban was subsequently selected as it could be sensitively detected.

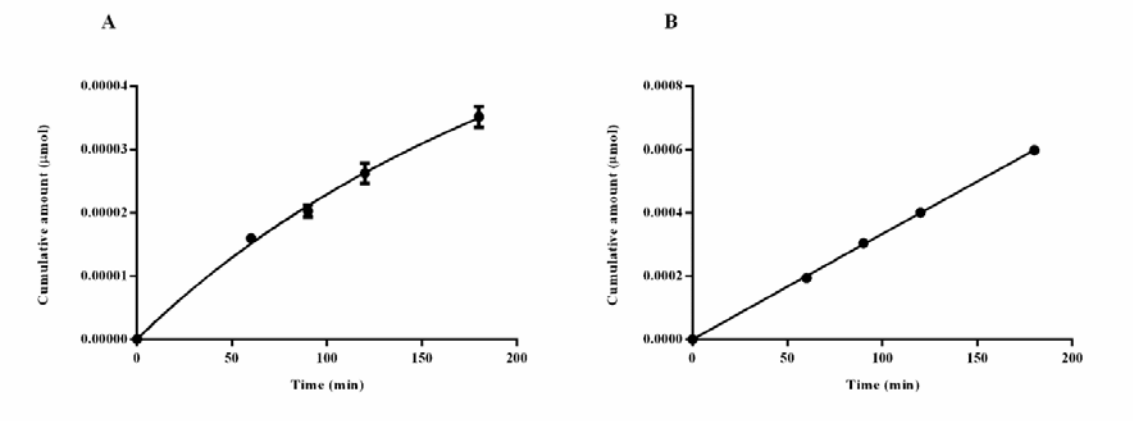

Supplemental Figure 1. Time-dependent (A) A→B and (B) B→A transport of rivaroxaban (10 µM). The gradients of the graphs represent dQ/dt, the flux of rivaroxaban across MDCK-MDR1. Both graphs were fitted with nonlinear regression Michaelis Menten models. Each point in (A and B) represents the mean and S.D. of triplicate experiments.

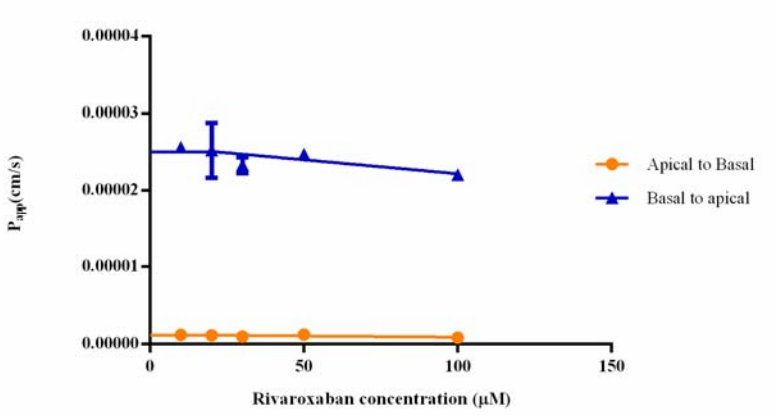

Supplemental Figure 2. Concentration dependent A→B and B→A transport of rivaroxaban (10 to 100 µM). Each point represents the mean and S.D. of triplicate experiments.

Sample processing for P-gp transport studies. For amprenavir and rivaroxaban samples, calibration standards and controls, the samples were spiked with 2 µL of 50 µM verapamil and subjected to a 2-step liquid-liquid extraction (LLE). In the first extraction, 1 ml of methyl tert butyl ether (MTBE) was aliquoted into each tube and vortexed at high speed for 5 min. Samples were then centrifuged using a microfuge at 10 000 g for 5 min at 4 °C to ensure complete separation of the media from the extraction solvent. 800 µL of MTBE was carefully aliquoted from each tube to a corresponding 2 mL

Eppendorf tube. For the second extraction, another 500 µL of MTBE was added, vortexed and spun down in a similar manner before 600 µL of MTBE was aliquoted and added to the same corresponding tube. The extraction solvent was then dried down in a turbovap using nitrogen gas at 3-5 psi before reconstituting in 200 µL of 0.1% formic acid in 50 % ACN/methanol for rivaroxaban and 0.1% formic acid in methanol for amprenavir. The sample processing for propranolol followed a similar protocol except the extraction solvent used was 30% ethyl acetate in MTBE. The samples were then transferred to vials for LC/MS/MS analysis.

LC/MS/MS quantitation. A calibration curve was built using 0.01, 0.1, 0.25, 0.5, 0.75, 1, 2, 3, 4, 5, 10 µM of rivaroxaban reconstituted in 50% ACN/methanol in DMEM. To measure accuracy, quality control (QC) samples were prepared in triplicates using a similar method where low, medium and high QCs were 0.125, 2.5 and 7.5 µM respectively. Each standard and QC was also spiked with 2µl of 50µM verapamil as internal standard. To account for chemical degradation that might have occurred during the cell assay, the calibrants were exposed at room temperature for 90 min similar to test samples. Both calibrants and QCs were subjected to the same sample processing method.

The LC/MS/MS system was similar to that described before. The sample injection volume was 1 µL for rivaroxaban, amprenavir and propranolol. Solvent A composed of 0.1% [v/v] formic acid in MiliQ water while solvent B composed of 0.1% [v/v] formic acid in acetonitrile. The solvents were pumped into the column at a flow rate of 0.6 mL/min. The gradient program for rivaroxaban was as follows: linear gradient from 25% to 95 % B (0-1.21 min), isocratic at 95% B (1.21-2 min), linear gradient from 95% to 25% B (2-2.01 min) and isocratic at 25% B (2.01-2.5 min). To prevent compound accumulation on the needle, 50 % methanol in ACN was used as needle wash for 30 s per sample. For amprenavir, the gradient program was: linear gradient from 20% to 25% B (0-1.00 min), 25% to 40% B (1.00-1.5 min), 40% to 50% B (1.5 – 2 min), isocratic at 50% B (2-2.5 min), linear gradient from 50% to 95% B (2.5 – 2.51 min), isocratic at 95% B (2.51 – 2.80 min), linear gradient 95% to 20% B (2.80 – 2.81 min) and isocratic at 20 % B (2.81 – 3 min). 100 % methanol was used as the needle wash for amprenavir. For propranolol, the gradient program was linear gradient from 25% to 30% B

(0-1 min), 30% to 35% B (1 – 1.2 min), 35% to 40% B (1.2 – 1.5 min), 40% to 50% B (1.5 – 1.75 min), 50% to 65% B (1.75 -2 min), 65% to 95% B (2 – 2.01 min), 95% to 25% B (2.01 to 2.3 min) and isocratic at 25% B (2.3 – 2.5 min). The MRM transition and compound dependent MS parameters of the analytes are summarized in **Supplemental Table 1**.

Calculation of apparent permeability, percentage recovery and efflux ratio. P_{app} (A→B, B→A) was calculated based on Equation 1, where *Q* is the amount of substrate (unit), C_0 is the concentration at $t = 0$ s, SA is the surface area (cm^2) and *t* is the incubation time (s).

$$P_{app} of\ substrate\ (\frac{cm}{s}) = \frac{dQ/dt}{C_0 \times SA} \quad (1)$$

The percentage recovery of a drug from one chamber to the other chamber was calculated based on Equation 2, where D_{90} is the amount of substrate at donor chamber at $t = 90$ min (unit), R_{90} is the amount of substrate at receiver chamber at $t = 90$ min (unit) and D_0 is the amount of substrate at donor chamber at $t = 0$ min (unit).

$$Percentage\ recovery\ (\%) = \frac{D_{90} + R_{90}}{D_0} \quad (2)$$

Efflux ratio, defined as the ratio of P_{app} (B→A) to P_{app} (A→B), was calculated using Equation 3 where P_{app} (B→A) is the apparent permeability of substrate from B to A (cm/s) and P_{app} (A→B) is the apparent permeability of substrate from A to B (cm/s).

$$Efflux\ ratio = \frac{P_{app}\ (B \rightarrow A)}{P_{app}\ (A \rightarrow B)} \quad (3)$$

The efflux ratio data was subsequently processed by non-linear regression analysis using GraphPad PRISM® software version 6.01 (San Diego, CA, USA).

Supplemental Table 1: MRM transition and compound-dependent MS parameters of various analytes.

Compound	MRM Transition (*m/z*)	Collision Energy (CE) (*V*)	Declustering Potential (DP) (*V*)	Entrance Potential (EP) (*V*)	Collision Exit Potential (CXP) (*V*)
Hydroxylated Rivaroxaban	452.000 → 147.100	45	150	8	9
Amprenavir	506.220 → 245.200	20.160	169	7.7	10.510
Rivaroxaban	436.000 → 145.000	32	136	8	9
Propranolol	260.300 → 56.100	9.48	98.8	13.77	45.060
Verapamil	455.000→ 165.000	34	80	10	10

Supplemental Table 2. Drug-dependent parameters for determination of relevant *in vivo* concentrations of amiodarone, dronedarone and their metabolites.

	Amiodarone	**NDEA**	**Dronedarone**	**NDBD**
D, mg	400[1]	NA	800	NA
MW, g/moL	645.32	617.25	556.76	500.66
$C_{ss,max}$ (µg/L)	1930[1]	1790[1]	85-150[4] (Ave: 117.5)	107[5]

$f_{u,p}$	0.03[2]	0.02[2]	0.003[b]	0.015[b]
B/P	0.73[3]	3.3[3]	1	0.71[c]
k_a, h^{-1}	0.3[3]	NA	0.53[c]	NA
F_{oral}	0.35[1]	NA	~0.15[4]	NA
f_a	0.6[3]	NA	0.79[c]	NA
F_a [a]	0.4	NA	0.79	NA
E_H	0.13[1]	NA	0.82[d]	NA

B/P, blood to plasma partition ratio; D, total daily oral dose of the inhibitor; E_H, hepatic extraction ratio; F_{oral}, oral bioavailability, f_a, fraction of dose absorbed into the gut wall; F_a, product of the fractions absorbed and escaping intestinal metabolism; k_a, first order absorption rate constant

[a] Calculated using the equation $F_{oral} = f_a \times F_G \times F_H = f_a \times F_G \times (1 - E_H)$ where f_a is the fraction of the dose entering the cellular space of the enterocytes, F_G is the fraction of the drug entering the enterocytes that escapes first pass intestinal metabolism and F_H is the fraction of the drug entering the liver that escapes first pass hepatic metabolism and/or biliary secretion

[b] Reported by PubChem

[c] Predicted using physicochemical properties of the drug

[d] Predicted with *in vitro to in vivo* extrapolation using Simcyp's *in vitro* analysis toolkit

Derivation of F_G of rivaroxaban.

Plasma clearance after intravenous administration: 10 L/h[6]

Fraction excreted unchanged (f_e): 0.36[6]

Hepatic clearance = $(1 - 0.36) \times 10\ L/h$

$= 6.4\ L/h$

Human plasma to blood partition coefficient is 1.40 averaged[7]

$$CL_{H,b} = 6.4 \times 1.40 = 8.96\ L/h$$

$$E_H = \frac{CL_{H,b}}{Q_{H,b}}$$

$$E_H = \frac{8.96}{87} = 0.103$$

Where $CL_{H,b}$ is the hepatic blood clearance obtained by correcting plasma clearance after iv administration with blood:plasma ratio, $Q_{H,b}$ is the hepatic blood flow

F_a and F_G was corrected for F_a when data was available, otherwise complete absorption was assumed, as permeability is known to be high

Oral bioavailability ~80-100% with the administration of a 10 mg tablet

$$F = F_a \times F_G \times (1 - E_H)$$

$$0.8 = 1 \times F_G \times (1 - 0.103)$$

$$F_G = 0.89$$

Results:

Absence of inhibitory effect of amiodarone and NDEA on CYP2J2 with rivaroxaban as probe substrate. In the preliminary study of reversible inhibition for CYP2J2, the plot of the amount of metabolite against rivaroxaban concentration was fitted using a competitive inhibition model as CYP2J2 was shown to have a single large active site where most of its enzymatic activity occurred.[6] When tested for competitive inhibition, (**Supplementary Figure 3A**) high concentrations of both amiodarone and NDEA were easily overcome with a small increase in rivaroxaban concentration. Amiodarone demonstrated a lack of mechanism based inactivation (MBI) with CYP2J2. MBI can be characterized based on the presence of time-dependent inactivation, where plotting the natural logarithm of the percentage of enzyme activity remaining versus the pre-incubation time would yield a negative slope (k_{obs}).[13] Time-dependent inactivation was not demonstrated in preliminary studies of MBI of CYP2J2 with both amiodarone and NDEA (**Supplemental Figure 3B**). In order to ascertain that lack of inhibition was not confounded by weak enzymatic activity, an assay using a high concentration of amiodarone 50μM along with dronedarone 3μM was used. As MBI of dronedarone was reproduced successfully, it was confirmed that amiodarone demonstrated no time-dependent inactivation (**Supplemental Figure 3C)**.

It was thus concluded that both amiodarone and NDEA did not inhibit CYP2J2 when rivaroxaban was used as the probe substrate.

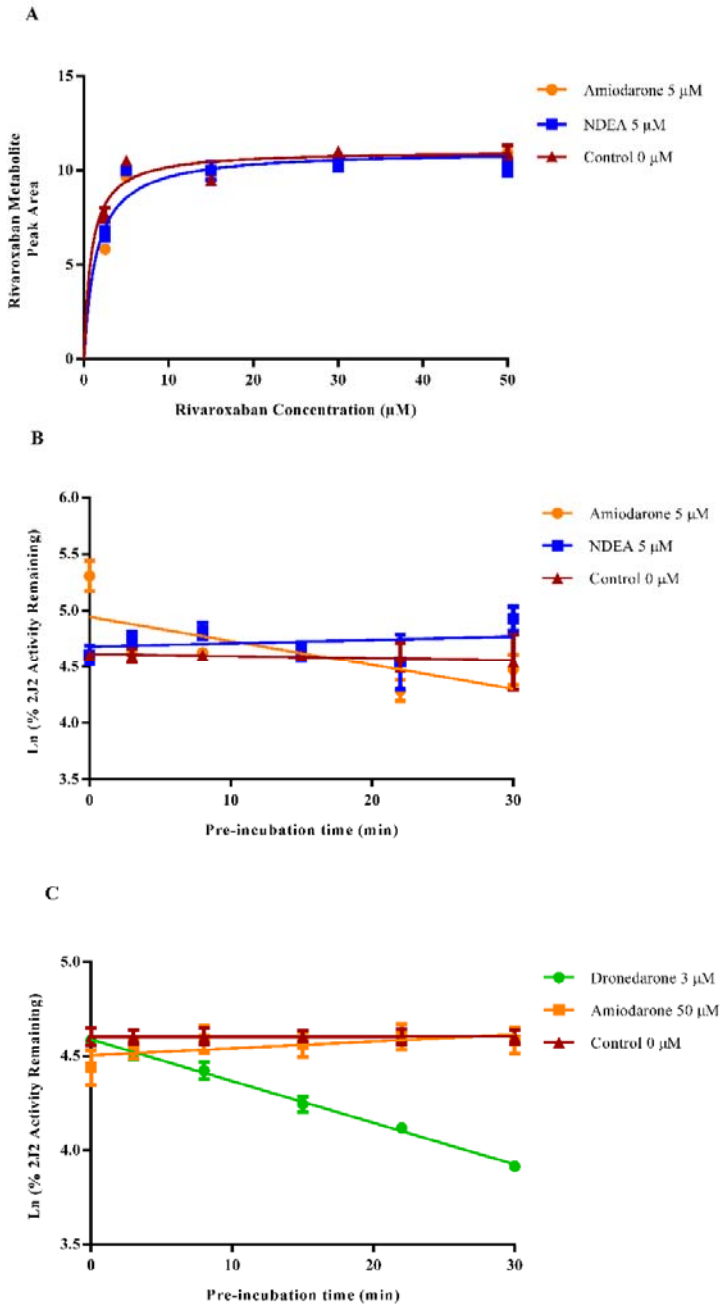

Supplemental Figure 3. (A) Competitive inhibition of CYP2J2 using 5 µM amiodarone and 5 µM NDEA; (B) Mechanism based inactivation of CYP2J2 by 5 µM amiodarone and 5µM NDEA and (C) Mechanism based inactivation of CYP2J2 by 50 µM amiodarone and 3 µM dronedarone (positive control). Each point represents the mean of triplicates.

Supplemental Table 3. Inactivation efficiency of dronedarone and NDBD against CYP3A4 and CYP2J2 in the presence of different probe substrates.

	k_{inact}/K_I (min^{-1}/mM^{-1})	
	Testosterone	**Rivaroxaban**
Dronedarone	44.8	185
NDBD	15.9	53.7

Supplemental References:

1. Holt DW, Tucker GT, Jackson PR, and Storey GC (1983) Amiodarone pharmacokinetics. *Am Heart J* 106:840–847.
2. McDonald MG, Au NT, Wittkowsky AK, and Rettie AE (2012) Warfarin-amiodarone drug-drug interactions: determination of [I](u)/K(I,u) for amiodarone and its plasma metabolites. *Clin Pharmacol Ther* 91:709–717
3. Chen Y, Mao J and Hop CE (2015) Physiologically based pharmacokinetic modeling to predict drug-drug interactions involving inhibitory metabolite: a case study of amiodarone. *Drug Metab Dispos* 43(2):182-9.
4. US FDA (2009a) MULTAQ (dronedarone) executive summary.
5. US FDA (2009b) MULTAQ (dronedarone) clinical pharmacology and biopharmaceutics review.
6. Mueck, W., Stampfuss, J., Kubitza, D. & Becka, M. (2014) Clinical pharmacokinetic and pharmacodynamic profile of rivaroxaban. *Clin Pharmacokinet* 53: 1–16.
7. Grillo, J. A. et al. (2012) Utility of a physiologically-based pharmacokinetic (PBPK) modeling approach to quantitatively predict a complex drug-drug-disease interaction scenario for rivaroxaban during the drug review process: implications for clinical practice. *Biopharm. Drug Dispos* 33: 99–110.